

## Using Charge Asymmetries to Measure Single Top Quark Production at the LHC

Matthew T. Bowen  
 Department of Physics, PO Box 351560,  
 University of Washington, Seattle, WA 98195, U.S.A.  
 [mtb6@u.washington.edu]

Electroweak production of single top quarks is an as-yet-unverified prediction of the Standard model, potentially sensitive to new physics. Two of the single top quark productions channels have significant charge asymmetries at the LHC, while the much larger background from  $t\bar{t}$  is nearly charge-symmetric. This can be used to reduce systematic uncertainties and make precision measurements of single top quark production.

PACS numbers: 13.85.Ni, 13.85.Qk

## ELECTROWEAK PRODUCTION OF SINGLE TOP QUARKS

The electroweak production of single top quarks at hadron colliders [1] is an important prediction of the Standard Model which remains to be verified. Limits from Run I at the Tevatron have been published [2], and new limits from Run II are just now emerging [3]. Measuring single top quark production is important because it equates to the first direct measurement of the CKM matrix element  $V_{tb}$ . In addition, anomalous top quark couplings and a variety of proposed new physics models affect the three single-top-quark production modes in largely orthogonal ways. Thus, independent measurements of all three channels provide a possible window to new physics [4], as well as for some discrimination between possible models.

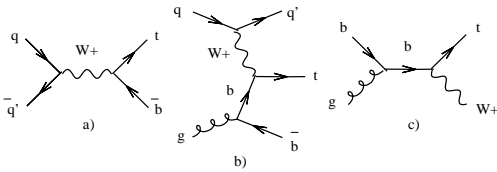


FIG. 1: Feynman diagrams for a)  $tb$ , b)  $tbq$ , and c)  $tW$  single top production.

One single-top-quark production mode, “ $tb$ ”, occurs through diagrams such as Figure 1a, where an  $s$ -channel  $W$  boson creates a top-bottom quark pair. A second, the so-called “ $W$ -gluon fusion” or “ $tbq$ ”, mode occurs through diagrams such as Figure 1b, where a  $t$ -channel  $W$  boson fuses with a bottom quark from gluon splitting to form a top. The “ $tW$ ” production mode [5] occurs when a bottom quark and a gluon scatter to create a top quark and a real  $W$  boson, as in Figure 1c. This last mode, which is smaller than  $tbq$ , but larger than  $tb$ , is

cleanly removed by the method outlined below, and will not be discussed at length.

The detector signature for  $tb$  and  $tbq$  single-top production comes primarily from the decay products of the top quark: one lepton, missing energy transverse to the beam (MET) from a neutrino, and one  $b$  quark — all at high  $p_T$ . In addition, the  $tb$  channel has a second large- $p_T$   $b$  quark, while the  $tbq$  channel has both a low- $p_T$   $b$  quark from gluon splitting, which is rarely visible, and a moderately high- $p_T$  light quark. After showering and hadronization, short-distance quarks and gluons lead to “jets” of energy in detector calorimeters. To reduce backgrounds, at least one jet in single top event selection samples is usually required to be “ $b$ -tagged” (identified as containing a metastable hadron, probably with a  $b$  quark constituent.)

At the LHC, the largest background to the  $tb$  and  $tbq$  signal is  $t\bar{t}$  pair production [6], where one or both of the top quarks decays leptonically, but only one lepton is identified. These events also have high- $p_T$  jets from  $b$  quarks, and typically one or two other high- $p_T$  jets from light quarks. A second background is  $W$  boson production with associated jets. For the present paper, this background will be divided into two sets:  $Wb\bar{b}$ , where the  $b$ -tags come from  $b$  quarks produced perturbatively in the hard scattering; and  $Wjj$ , where the  $b$ -tags come from mistagging of charm, gluon, and light quark jets, and also the fragmentation of short-distance gluons to  $b\bar{b}$  pairs. A third background comes from pure QCD processes, where a lepton is either misidentified or comes from the decay of a heavy-quark meson. The MET for these QCD events comes from jet energy fluctuations in the calorimeter. This background is not estimated here, but is argued to be small for the method described below.

The definitive signal-to-background study of single top quark production at the LHC has remained reference [6] since its publication. The size of the  $t\bar{t}$  background led the authors of [6] to study a “jet veto”, wherein events

with more than 2 jets were rejected. As  $t\bar{t}$  typically has more than 2 jets per event, the jet veto removed greater than 90% of this background. For the single  $b$ -tag sample, this technique was sufficient to study the  $tbq$  channel. For the double  $b$ -tag sample, however, the jet veto could not sufficiently reduce  $t\bar{t}$  to permit a study of either the  $tbq$  or  $tb$  channels.

### Charge Asymmetries

Fortunately, single top quark production is a very unusual process, with other features that can be used to separate it from backgrounds. At the Tevatron, single-top production has significantly larger parity asymmetries than its Standard Model backgrounds which can be used to help isolate the single top signal [10]. This is a result of the parity-asymmetric  $p\bar{p}$  initial state at the Tevatron, versus the charge-asymmetric  $pp$  initial state at the LHC. At the LHC, single-top production has large charge asymmetries which can be used to separate it from backgrounds. For both the  $tb$  and  $tbq$  channels, roughly 60 – 70% more top quarks are produced at the LHC than anti-top quarks, and this difference is preserved in the charge of the leptons from the top quark decays.

Define  $N_+$  ( $N_-$ ) to be the number of events with one high- $p_T$  positively- (negatively-) charged lepton. Then define  $N_{total} = N_+ + N_-$ ,  $\Delta = N_+ - N_-$ , and a charge asymmetry  $A_C = \Delta/N_{total}$ . For the cuts defined in table I, the  $tbq$  channel has a charge asymmetry of order 26% and is the largest contributor to  $\Delta$ . The  $tb$  channel has a charge asymmetry of order 20%, but, because of its much smaller cross-section, does not contribute as significantly to  $\Delta$ .

To first approximation, the  $t\bar{t}$  background has a charge asymmetry of zero. But  $N_+$  and  $N_-$  are functions of both the event kinematic distributions and the acceptance regions of the detectors. At leading-order (LO), the  $t$  and  $\bar{t}$  distributions are identical, but at NLO there is a preference for  $\bar{t}$  quarks to be more central than  $t$  quarks [11], so more  $t\bar{t}$  events with leptons ( $N_-$ ) will be detected than with anti-leptons ( $N_+$ ). However, the magnitude of this asymmetry is estimated below to be smaller than 0.05%.

QCD backgrounds should have smaller charge asymmetries than  $t\bar{t}$ . For example, the  $b\bar{b}$  background has smaller NLO corrections to its distributions than  $t\bar{t}$  [11]. In addition, neutral  $B$ -meson mixing dilutes the charge correlation between the  $b$  quarks and leptons, further reducing the contribution to  $\Delta$ . And to the extent that fake leptons from other QCD processes are charge symmetric, these also should not contribute significantly to  $\Delta$ .

The  $W$ +jets background, on the other hand, is more complicated. The sub-channels for this background do

have significant asymmetries of varying magnitudes and signs. This will be discussed further below, but the size and uncertainty of this background's contribution to  $\Delta$  do not appear to be prohibitively large.

Finally, the  $tW$  production mode is charge-symmetric because the  $b$  and  $\bar{b}$  parton distribution functions (PDFs) are believed to be charge-symmetric. There are also no known higher-order corrections to the kinematic distributions that would introduce a measurable charge asymmetry for this mode, and any future corrections are anticipated to be small. Thus, considering charge asymmetries provides a clean way of separating the  $tbq$  and  $tb$  modes from the  $tW$  mode.

### SIGNAL AND BACKGROUND STUDY

For the study below, MadEvent [12] is used to generate both signal and background event samples with the CTEQ5 [13] PDF set. Single top  $tb$  events are generated with  $\mu_F = \mu_R = m_t = 175$  GeV (where  $\mu_F$  and  $\mu_R$  are the factorization and renormalization scales) and normalized to 6.55 (4.07) pb [14] for  $t\bar{b}$  ( $t\bar{b}$ ) production. The  $tbq$  event set is generated using the same scales as [6]:  $\mu_F^2 = -q_W^2$  (where  $q_W$  is the t-channel W boson momentum) for the initial state quark PDF, and  $\mu_R^2 = \mu_F^2 = m_b^2 + p_{Tb}^2$  for the initial state gluon PDF.

At NLO, the  $tbq$  channel receives large contributions when the  $b$  or  $\bar{b}$  quark from gluon-splitting is at low  $p_T$ . In order to reflect this enhancement in a lowest-order (LO) simulation, reference [6] normalized the  $tbq$  sample differentially depending on the  $p_T$  of the  $b$  or  $\bar{b}$  from gluon-splitting (from here on, the  $b$  or  $\bar{b}$  is referred to simply as “the  $b$  quark”). In [6], the cross-section with the  $b$  quark  $p_T$  above 20 GeV was determined at LO to be 81 pb, and the cross-section with the  $b$  quark  $p_T$  below 20 GeV was normalized to 164 pb to match the total NLO cross-section of 245 pb [7].

References [6] and [7] were not concerned with separating the  $tbq$  and  $\bar{t}bq$  channels, so only the sum of the two was quoted. They are separated here by computing the ratio of the LO  $tbq$  and  $\bar{t}bq$  cross-sections with the  $b$  quark  $p_T$  above 20 GeV using MadEvent [12], and multiplying by 81 pb [6]. For the  $b$  quark  $p_T$  above 20 GeV, this leads to 52 pb for  $t\bar{b}q$  and 29 pb for  $\bar{t}bq$ . The  $\bar{t}bq$  sample with the  $b$  quark  $p_T$  below 20 GeV is normalized to 104 pb, so that when added to 52 pb, the total  $\bar{t}bq$  cross-section is equal to the total NLO rate of 156 pb [14]. Likewise, the  $t\bar{b}q$  sample with the  $b$  quark  $p_T$  below 20 GeV is normalized to 62 pb to match the total NLO rate of 91 pb [14]. Note that the quoted total  $tbq$  cross-sections in [7] and [14] differ by 1%, which is negligible for the current analysis.

The  $t\bar{t}$  sample is generated with  $\mu_R = \mu_F = m_t$  and normalized to 873 pb [15]. The  $Wb\bar{b}$  and  $Wjj$  sets are generated with  $\mu_F = \mu_R = M_W$  and normalized with K-

Item	$p_T$	$ \eta $
$\ell^\pm$	$\geq 20$ GeV	$\leq 2.5$
MET ( $\nu$ )	$\geq 20$ GeV	-
$b$ -tagged jets	$\geq 30$ GeV	$\leq 2.5$
other jets	$\geq 30$ GeV	$\leq 4.5$

TABLE I: Detector cuts used to select events.

factors = 2.35 and 0.87 [8], respectively. These K-factors are taken from the study done in [8], under the assumption that they are the same for the slightly different cuts used here. The  $W$ +jets background is only simulated for  $W$ -plus-two jets, since the uncertainty in this prediction is probably as large as the  $W$ -plus-three jets contribution is likely to be.

Partons are mapped to jets by smearing their energies with a gaussian function of width  $\sigma/E = 0.64/\sqrt{E} \oplus 0.036$ , from Table 9-1 in [9], to simulate showering and detector response. Taus are treated as jets. Leptons are required to be separated from jets by  $\Delta R = 0.7$ , and jets within  $\Delta R = 0.7$  of each other are merged.

The  $b$ -tagging parametrizations for jets from bottom quarks, charm quarks, gluons, and light quarks are derived from Figure 10-24 of [9], which assumes that jets from  $b$  quarks are tagged at a fixed rate of 50%. Jets from charm quarks are tagged at an efficiency  $\epsilon_c(\%) = 7.26 + 123 \text{ GeV}/p_T + 0.0044 \text{ GeV}^{-1} \times p_T$ , gluons at  $\epsilon_g(\%) = -14.1 + 185 \text{ GeV}/p_T + 2.9 \times \ln(p_T/\text{GeV})$ , and light quarks at  $\epsilon_q(\%) = -1.5 + 71 \text{ GeV}/p_T + 0.0095 \times (p_T/\text{GeV})$ . For the  $W$ +jets sample, using the cuts in Table I, this is approximately equivalent to tagging charm quark, gluon, and light quark jets at fixed rates of 10%, 1.3%, and 0.5%, respectively.

For this study, events are required to have MET, one and only one charged lepton, and at least two jets, with one or two of them  $b$ -tagged. Table I lists the cuts used to select events, and Table II lists the cross-section in femtobarns (fb) for each channel after branching-ratios and detector cuts.

### The $t\bar{t}$ Asymmetry

The asymmetry in  $t\bar{t}$  at NLO cannot currently be computed, since there is no NLO event generator for  $t\bar{t}$  which includes the spin correlations for top quark decay. For this paper, an upper bound on the magnitude of the observed charge asymmetry for  $t\bar{t}$  is estimated using Figure 14 in Reference [11]. This figure plots the  $t\bar{t}$ -pair charge asymmetry  $A_{t\bar{t}}(y)$  for  $q\bar{q}$  initial-states as a function of rapidity. If the detector has acceptance in the rapidity range  $-y_o < y < y_o$ , the total asymmetry observed for

Channel	1 tag	2 tags
$t\bar{b}$	277	106
$\bar{t}b$	178	73
$t\bar{b}q$	7,410	955
$\bar{t}bq$	4,300	552
$W^+b\bar{b}$	1,340	531
$W^-b\bar{b}$	858	351
$W^+jj$	12,700	79
$W^-jj$	10,900	76
$t\bar{t}$	95,700	33,600

TABLE II: Cross-sections (in femtobarns) with 1 or 2  $b$ -tags required, after accounting for leptonic branching ratios and detector cuts.  $Wjj$  includes all final states with charm quarks, gluons, and light quarks.

$q\bar{q}$  initial states is:

$$A_{q\bar{q}}(y_o) = \frac{\int_{-y_o}^{y_o} dy \frac{d\sigma_{t\bar{t}}}{dy}(y) \times A_{t\bar{t}}(y)}{\int_{-y_o}^{y_o} dy \frac{d\sigma_{t\bar{t}}}{dy}(y)} \quad (1)$$

As  $y_o \rightarrow \infty$ ,  $A_{q\bar{q}}$  goes to zero, as there are the same number of  $t$  and  $\bar{t}$  quarks. For  $y_o \rightarrow 0$ ,  $A_{q\bar{q}}$  goes to  $-0.25\%$ , the value of  $A_{t\bar{t}}(y)$  at  $y = 0$ . Since  $\frac{d\sigma_{t\bar{t}}}{dy}(y) > 0$ ,  $\frac{d\sigma_{t\bar{t}}}{dy}(y) = \frac{d\sigma_{t\bar{t}}}{dy}(-y)$ ,  $A_{t\bar{t}}(y) = A_{t\bar{t}}(-y)$ , and  $A_{t\bar{t}}(y)$  is monotonically increasing with  $|y|$  [11], any  $y_o$  will yield an asymmetry  $0 \geq A_{q\bar{q}} \geq -0.25\%$ .

Since there are no NLO corrections to  $gq$  initial states which introduce charge asymmetries, and the charge-asymmetric corrections to  $gq$  initial states are small enough to neglect [11], the overall bound on the  $t\bar{t}$  charge asymmetry can be estimated solely from this bound on  $A_{q\bar{q}}$ . At LO,  $q\bar{q}$  initial states account for less than 20% of the cross-section at the LHC, so the total observed asymmetry  $A_C$  for  $t\bar{t}$  is estimated to be in the range  $0\% > A_C \approx 0.2A_{q\bar{q}} > -0.05\%$ . This bound on the  $t\bar{t}$  asymmetry is used here as a surrogate for a bound on the observed lepton-antilepton asymmetry, which has not yet been studied. Because the  $t\bar{t}$  asymmetry is so small, this estimate can be off by a factor of two or more without becoming a problem for the measurement.

### Results

Table III shows that the signal-to-background ratio for the single-tag sample is 1:10 for the total number of events, but around 3:2 for  $\Delta$ . The contribution from  $t\bar{t}$  to  $\Delta$  is so small that even large systematic uncertainties in its prediction are not a problem. Further, even with only  $10 \text{ fb}^{-1}$ , the measurement of  $\Delta$  is not limited by statistics, at least with the cuts of Table I.

The conclusions for the double-tag sample, shown in Table IV, are much the same, except that statistical un-

Channel	$N_{total}$	$\Delta$	$\sqrt{N_{total}}$
$tb$	4,550	990	67
$tbq$	116,000	30,900	340
$Wb\bar{b}$	21,900	4,820	150
$Wjj$	236,000	18,000	490
$t\bar{t}$	958,000	-479	980
Total	1.34M	54,200	1,200

TABLE III: Numbers of events with 1  $b$ -tag for  $10 \text{ fb}^{-1}$ .  $t\bar{t}$  is assumed to have a  $-0.05\%$  charge asymmetry.

Channel	$N_{total}$	$\Delta$	$\sqrt{N_{total}}$
$tb$	1,790	330	42
$tbq$	15,100	4,030	120
$Wb\bar{b}$	8,800	1,800	94
$Wjj$	1,550	30	40
$t\bar{t}$	336,000	-167	580
Total	363,000	6,020	600

TABLE IV: Numbers of events with 2  $b$ -tags for  $10 \text{ fb}^{-1}$ .  $t\bar{t}$  is assumed to have a  $-0.05\%$  charge asymmetry.

certainties in  $t\bar{t}$ 's contribution to  $\Delta$  are more significant with only  $10 \text{ fb}^{-1}$  of data, though still manageable. On the other hand, the signal-to-background ratio for  $\Delta$  in the double-tag sample is 2:1, and is thus potentially even less sensitive to systematic errors than the single tag sample. With higher statistics, the double-tag sample could potentially be better than the single-tag sample for a study of single-top-quark production.

As this study has been done for a small dataset of  $10 \text{ fb}^{-1}$ , lower detector efficiencies than assumed here will not be problematic. In addition, larger  $p_T$  cuts on reconstructed objects do not decrease the charge asymmetry of the  $tbq$  channel. If conditions at the LHC dictate that all MET, jet  $p_T$ , and lepton  $p_T$  cuts must be raised to  $50 \text{ GeV}$ , the signal will be reduced by roughly  $90\%$  for the single-tag sample.

However, the charge asymmetry method is crucially sensitive to systematic uncertainties in effects which impact the  $N_+$  and  $N_-$  samples asymmetrically. For example, a systematic uncertainty in the efficiency of positively-charged lepton reconstruction of order  $0.5\%$ , which does not exist for the reconstruction of negatively-charged leptons, could lead to an uncertainty in the prediction of  $\Delta$  for  $t\bar{t}$  which is of the same order as the signal. Ensuring that these kinds of uncertainties are sufficiently small will require a detailed understanding of the detector response to leptons and antileptons.

This opportunity for studying single top quark production at the LHC should be contrasted with the cur-

rent reality at the Tevatron. Currently, there is no clear way to reduce the signal-to-background ratio to order unity at the Tevatron without problematic systematic and statistical uncertainties [10]. The LHC, on the other hand, will not be statistics limited, and systematic uncertainties can be controlled through the use of charge asymmetries. This should allow the LHC to make a precision test of the Standard Model via single top quark production.

### Acknowledgements

The author thanks S. Ellis, A. Haas, and M. Strassler for useful discussions and suggestions. This work was supported by U.S. Department of Energy grant DE-FG02-96ER40956.

- 
- [1] S. S. D. Willenbrock and D. A. Dicus, Phys. Rev. D **34**, 155 (1986). C. P. Yuan, Phys. Rev. D **41**, 42 (1990); S. Cortese and R. Petronzio, Phys. Lett. B **253**, 494 (1991); R. K. Ellis and S. J. Parke, Phys. Rev. D **46**, 3785 (1992); D. O. Carlson and C. P. Yuan, Phys. Lett. B **306**, 386 (1993); T. Stelzer and S. Willenbrock, Phys. Lett. B **357**, 125 (1995)
  - [2] D. Acosta *et al.* [CDF Collaboration], Phys. Rev. D **65**, 091102 (2002) [arXiv:hep-ex/0110067]. B. Abbott *et al.* [D0 Collaboration], Phys. Rev. D **63**, 031101 (2001) [arXiv:hep-ex/0008024].
  - [3] D. Acosta *et al.* [CDF Collaboration], [arXiv:hep-ex/0410058].
  - [4] T. Tait and C. P. Yuan, Phys. Rev. D **63**, 014018 (2001) [arXiv:hep-ph/0007298].
  - [5] T. M. P. Tait, Phys. Rev. D **61**, 034001 (2000) [arXiv:hep-ph/9909352].
  - [6] T. Stelzer, Z. Sullivan and S. Willenbrock, Phys. Rev. D **58**, 094021 (1998) [arXiv:hep-ph/9807340].
  - [7] T. Stelzer, Z. Sullivan and S. Willenbrock, Phys. Rev. D **56**, 5919 (1997) [arXiv:hep-ph/9705398].
  - [8] J. Campbell, R. K. Ellis and D. L. Rainwater, Phys. Rev. D **68**, 094021 (2003) [arXiv:hep-ph/0308195].
  - [9] ATLAS Technical Design Report, Vol. I, CERN/LHCC/99-14 (1999)
  - [10] M. T. Bowen, S. D. Ellis and M. J. Strassler, [arXiv:hep-ph/0412223].
  - [11] J. H. Kuhn and G. Rodrigo, Phys. Rev. D **59**, 054017 (1999) [arXiv:hep-ph/9807420].
  - [12] F. Maltoni and T. Stelzer, JHEP **0302**, 027 (2003) [arXiv:hep-ph/0208156].
  - [13] H. L. Lai *et al.* [CTEQ Collaboration], Eur. Phys. J. C **12**, 375 (2000) [arXiv:hep-ph/9903282].
  - [14] B. W. Harris, E. Laenen, L. Phaf, Z. Sullivan and S. Weinzierl, Phys. Rev. D **66**, 054024 (2002) [arXiv:hep-ph/0207055].
  - [15] N. Kidonakis and R. Vogt, Phys. Rev. D **68**, 114014 (2003) [arXiv:hep-ph/0308222].